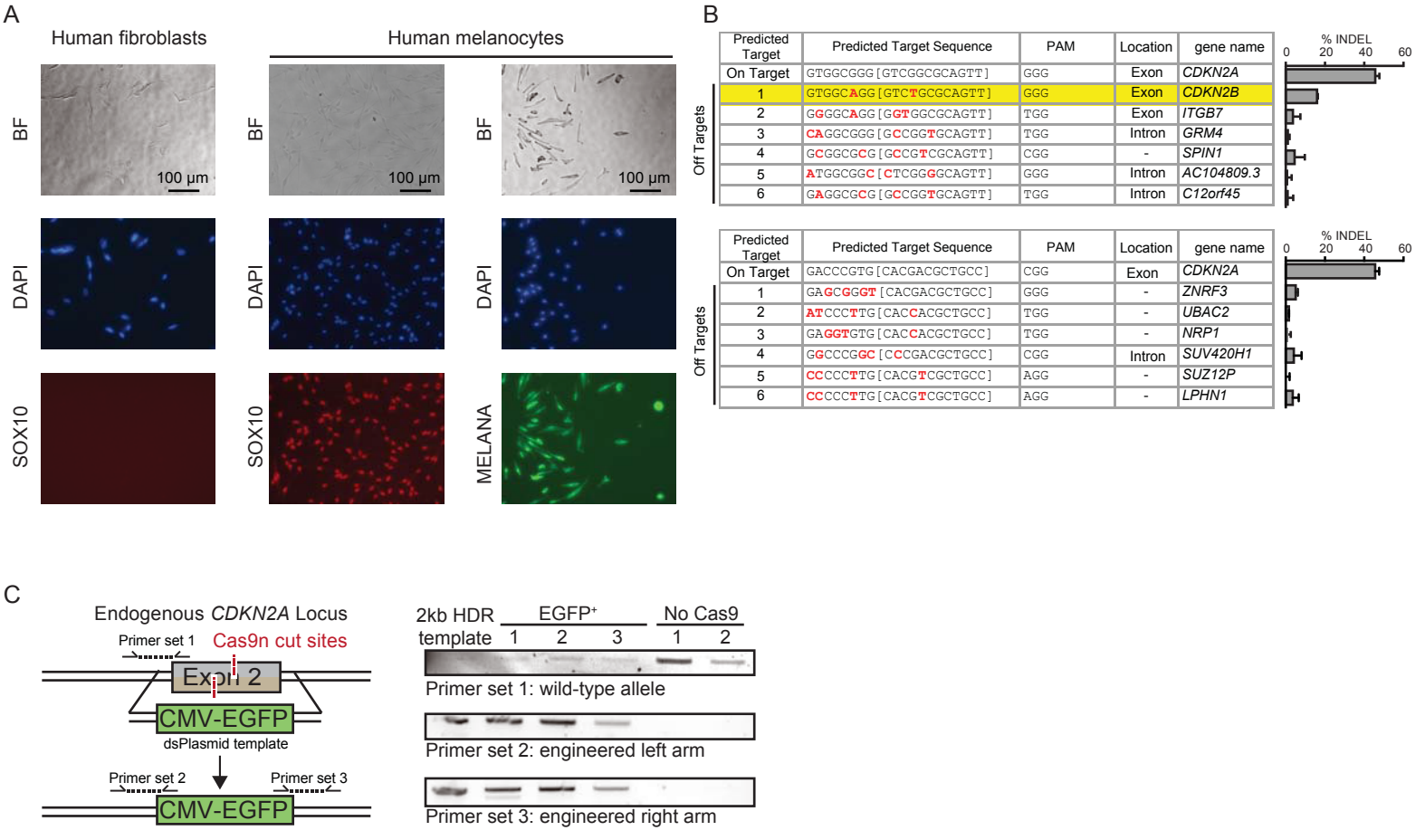

Figure S1. Validation of normal human melanocyte isolation and *CDKN2A* engineering, Related to Figure 1. (A) Immunofluorescent staining of primary low-passage human melanocytes for melanocyte-specific markers, SOX10 and MELANA. Primary low-passage human dermal fibroblasts are shown for comparison. (B) Table of the most likely off-target cutting sites for *CDKN2A* exon 2 sgRNA. Red letters indicate mismatches in critical (bracketed) or non-critical sequences. Bar graph indicates cutting efficiency at site measured by Tide (n=3). Highlighted off-target site indicates non-zero cutting efficiency. (C) Strategy for genotyping (left) and PCR results (right) for correct engineering ofmean for three transfections. *CDKN2A* exon2::CMV-EGFP. Error bars indicate standard deviation of the mean for three transfections.

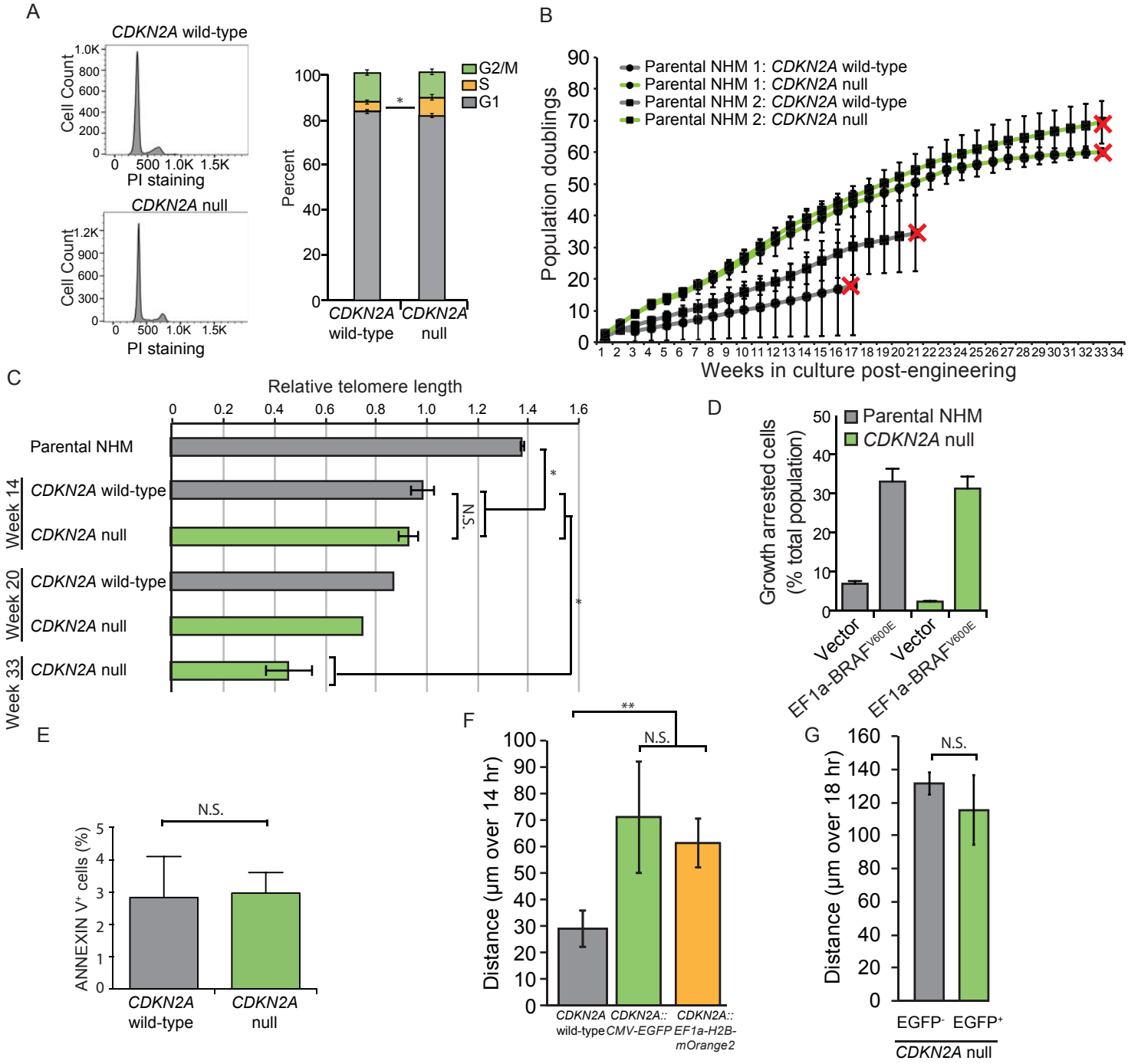

Figure S2: Comparison of cell behaviors between *CDKN2A* null NHMs and wild-type sibling cells, Related to Figure 2. (A) Representative cell cycle profiles of *CDKN2A* null NHMs and wild-type sibling cells (left) and quantification of three replicates (right). (B) Long term serial culture of *CDKN2A* null NHMs and wild-type sibling cells. Data represent three CRISPR reactions over on two preparations of primary NHMs (NHM1 and NHM2). Red Xs indicate termination of experiment due to insufficient cell survival from previous week. (C) RT-qPCR analysis of telomere length from sampling of cells in (B). Only one sample each was collected for week 20. (D) Percentage of growth-arrested *CDKN2A* null NHMs and wild-type sibling cells five days after transduction with EF1alpha-controlled mOrange2 (vector) or BRAF^{V600E}-IRES-mOrange2 (EF1a-BRAF^{V600E}). Data represent three infections. (E) Percentage of ANNEXIN V positive *CDKN2A* null NHMs and wild-type sibling cells. Data represent three engineered pairs. (F) Population motility analysis of *CDKN2A* null NHMs compared to wild-type siblings. NHMs were engineered with either a CMV-driven cytosolic EGFP or an EF1a-driven nuclear mOrange2 replacing *CDKN2A* exon 2. Data represent six CRISPR reactions of three preparations of NHMs. (G) Population motility analysis of high passage (p12) *CDKN2A* null NHMs. A subpopulation of engineered cells spontaneously silenced EGFP expression and were isolated via FACS. Motility between the two matched groups is compared. Data represent three experiments of a single matched pair. All error bars indicate standard deviation of the mean. Asterisks indicate p value of * <0.05 to ** <0.005 from unpaired t-test. N.S. indicates no significant difference.

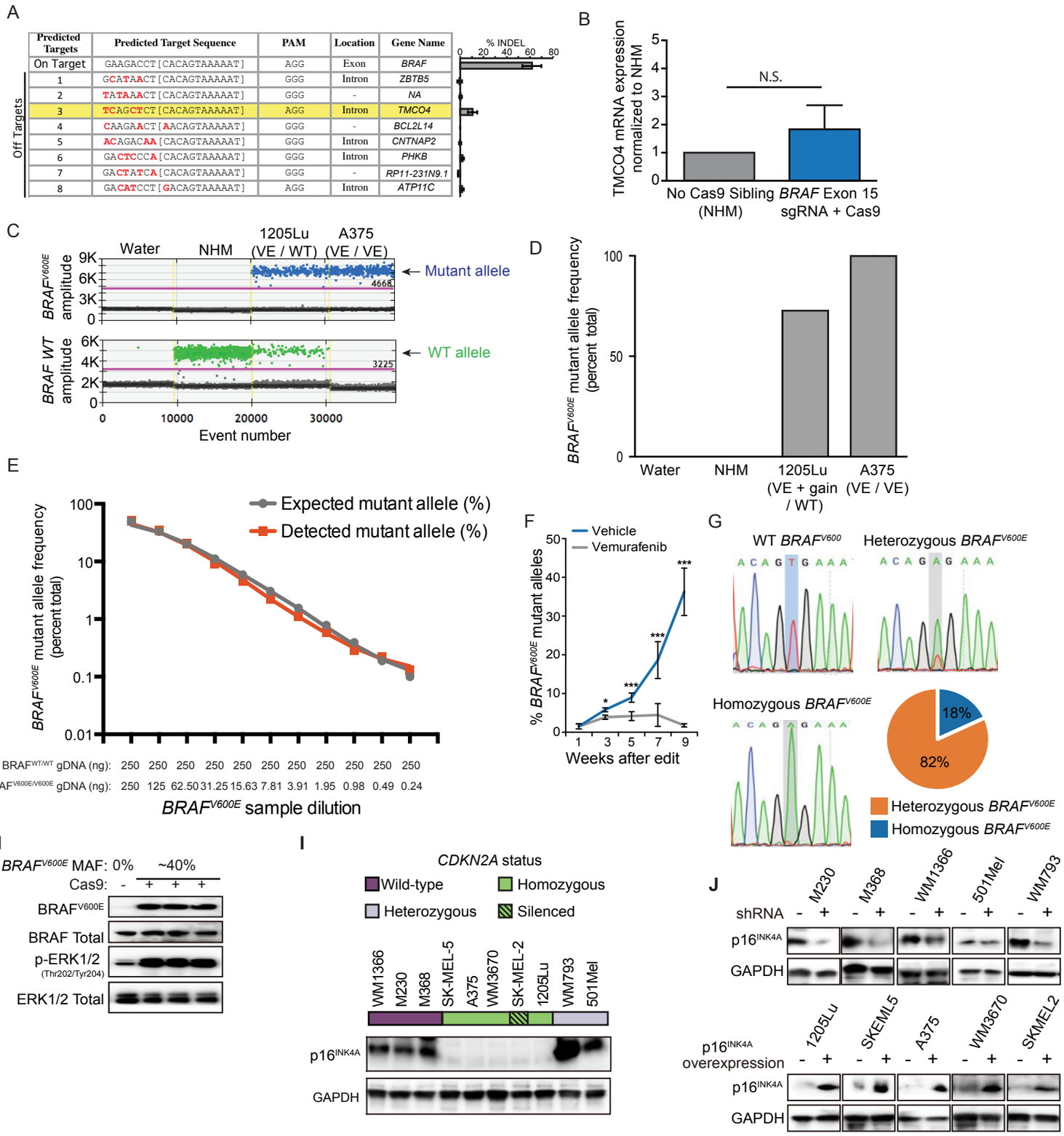

Figure S3. Validation of *BRAF*^{V600E} engineering and *CDKN2A* regulated motility on diverse genetic backgrounds, Related to Figure 3. (A) Table of the most likely off-target cutting sites for *BRAF* Exon 15 sgRNA. Red letters indicate mismatches in critical (bracketed) or non-critical sequences. Bar graph indicates cutting efficiency at site as measured by Tide (n=3). Highlighted off-target sites indicate non-zero cutting efficiency. (B) RT-qPCR measuring TMCO4 mRNA expression, which contains a large intron targeted at low frequency by *BRAF* Exon 15 sgRNA. No significant change in expression upon sgRNA transfection (n=3) was observed. (C) Specificity of *BRAF*^{V600E} and *BRAF*^{V600WT} dd-qPCR probes as tested in *BRAF*$^{WT/WT}$ cells (NHM), *BRAF*$^{V600E+gain/wt}$ cells (1205Lu) and *BRAF*$^{V600E/V600E}$ cells (A375). Each colored point represents a positive droplet. Droplets of single representative assay are quantified in (D). (E) Sensitivity of *BRAF*^{V600E} dd-qPCR probes, tested in dilution of *BRAF*$^{V600E/V600E}$ genomic DNA (A375) in *BRAF*$^{wt/wt}$ genomic DNA (NHMs). (F) Mutant allele frequency of engineered *BRAF*^{V600E} weeks after editing of NHMs in the presence and absence of 0.35μM vemurafenib, as measured by dd-qPCR. Data represent six CRISPR reactions of two preparations of NHMs. (G) Sanger sequencing chromatograms from clonal NHM populations. Shown are wild-type *BRAF* from non-engineered NHMs and mono-allelic and bi-allelic *BRAF*^{V600E} from edited NHMs. Pie chart shows distribution of genotyping from eleven clonal populations isolated from edited NHM populations that had reached 50% MAF for the *BRAF*^{V600E} allele. (H) Western blot analysis of mutant and total BRAF and ERK activation in three independently edited NHM populations grown to 40% MAF for the *BRAF*^{V600E} allele. (I) Western blot analysis of p16^{INK4A} status of the ten human melanoma lines analyzed in Figure 3D. (J) Western blot analysis of p16^{INK4A} manipulation in the ten human melanoma lines analyzed in Figure 3E-F. All error bars indicate standard deviation of the mean. Asterisks indicate p value of * <0.05 to *** <0.0005 from unpaired t-test. N.S. indicates no significant difference.

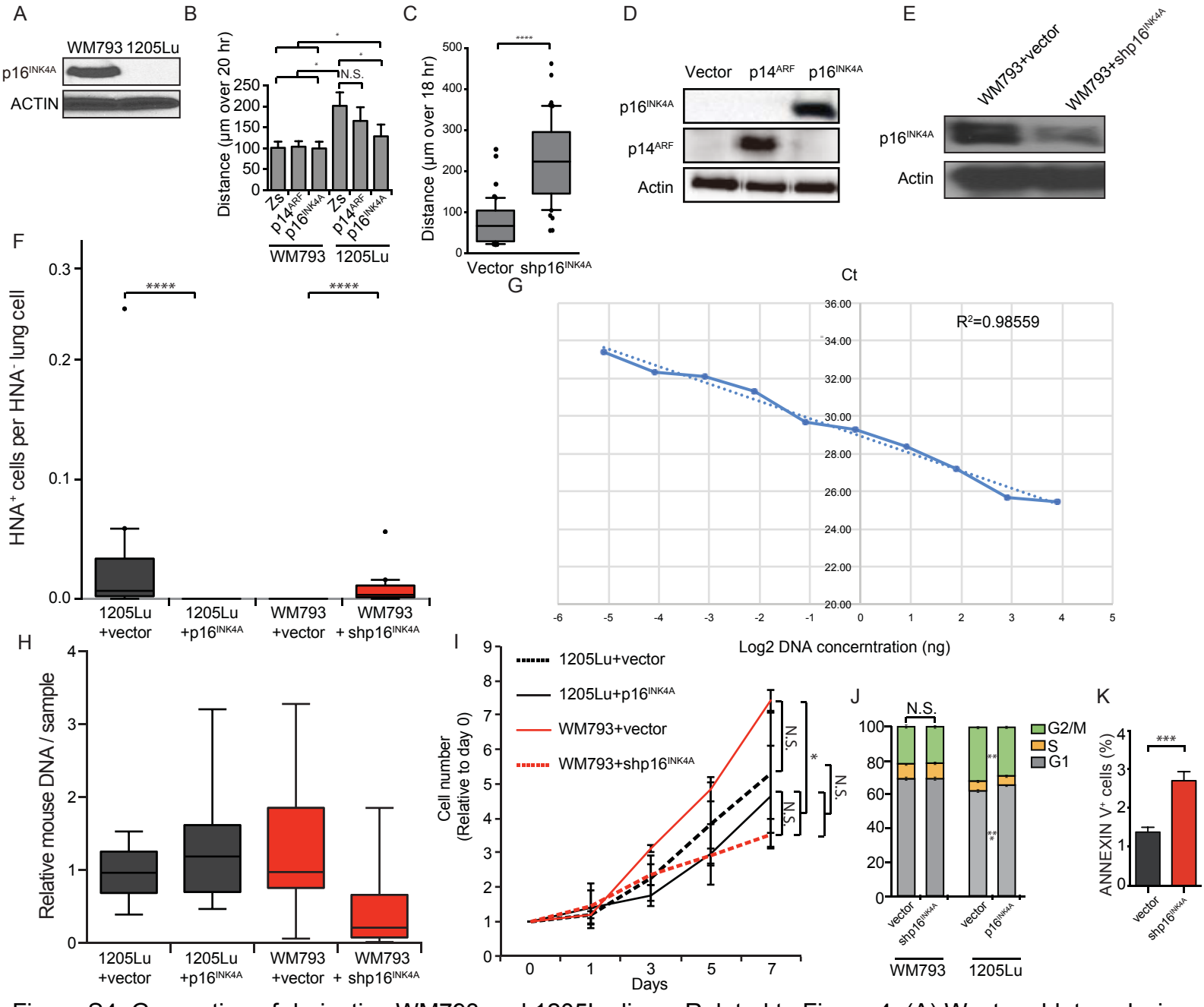

Figure S4. Generation of derivative WM793 and 1205Lu lines, Related to Figure 4. (A) Western blot analysis p16^{INK4A} expression in WM793 and 1205Lu lines. (B) Motility analysis of WM793 and 1205Lu cells transduced with and sorted for vectors expressing zsGreen (Zs), p14^{ARF}-IRES-zsGreen (p14^{ARF}) or p16^{INK4A}-IRES-zsGreen (p16^{INK4A}). Data represent three separate infections. (C) Single cell motility analysis of at least fifty single WM793 cells transduced with and sorted for either pSICOR-mCherry (vector) or pSICOR-shp16^{INK4A}-mCherry. (D) Western blot validation of p16^{INK4A} and p14^{ARF} overexpression from (B). (E) Western blot validation of p16^{INK4A} knock-down from (C). (F) Quantification of IF images from Figure 4E, showing the number of HNA positive cells in the lung normalized to the number of HNA negative cell in the lung for each condition (each bar represents 100 quantified sections over 5 mice covering over 14,000 cells per condition). (G) Representative standard curve for calculating absolute levels of human genomic DNA from CT values in Figures 4H and 5E. A curve was generated on each qPCR plate using dilutions of known amounts of human genomic DNA and the identical primer set used in the experiments. (H) Relative levels of mouse genomic DNA from samples in Figure 4H. (I) The effect of p16^{INK4A} knockdown and overexpression on cell line proliferation in vitro. Data represent three independent transductions and FACS-isolations. (J) The effect of p16^{INK4A} knockdown or overexpression on WM793 or 1205Lu cell cycle respectively. Data represent four experiments. (K) The effect of p16^{INK4A} knockdown on WM793 the apoptosis marker, ANNEXIN V. Data represent three experiments. All box and whisker plots represent mean, 10th, 25th, 75th & 90th percentiles. All error bars represent standard deviation of the mean. Asterisks indicate p-values of * <0.05 to **** <0.00005 from unpaired t-test. N.S. indicates no significant difference.

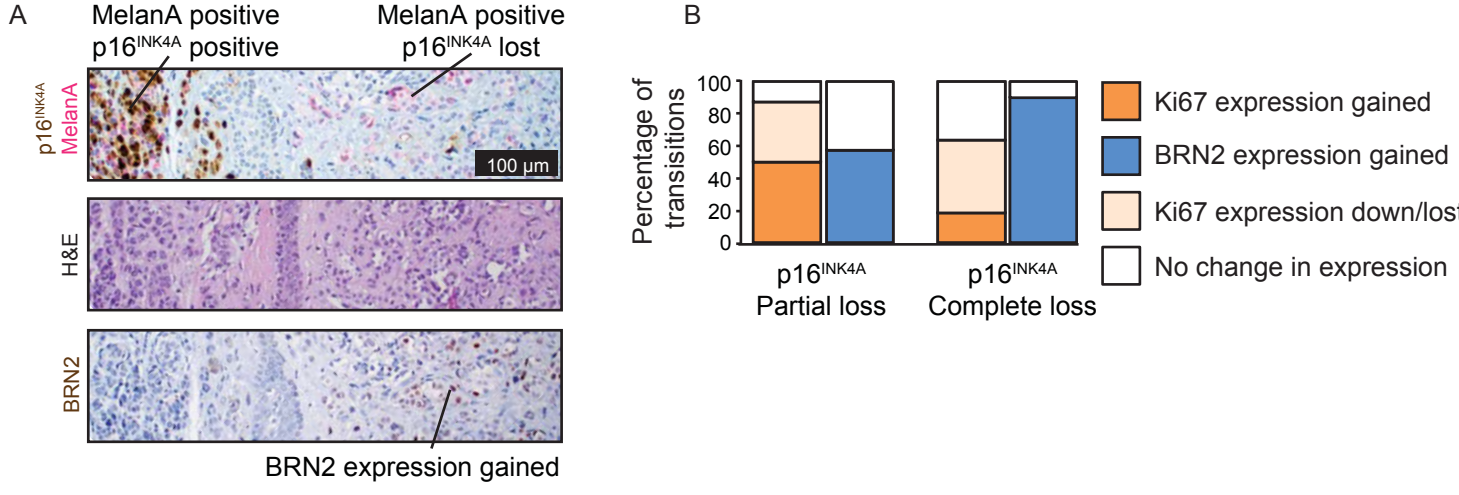

Figure S5: Relationship between p16^{INK4A} and BRN2 protein expression, Related to Figure 6. (A) Example case of MelanA positive transition lesion categorized as complete loss of p16^{INK4A} with associated gain of BRN2 expression. (B) Quantification of change in BRN2 or Ki67 IHC staining in adjacent MelanA positive regions presenting differential p16^{INK4A} staining. Differential p16^{INK4A} staining was categorized as either partial loss (visible in both adjacent regions, but lower in one) or complete loss (visible in only one of the two adjacent regions).

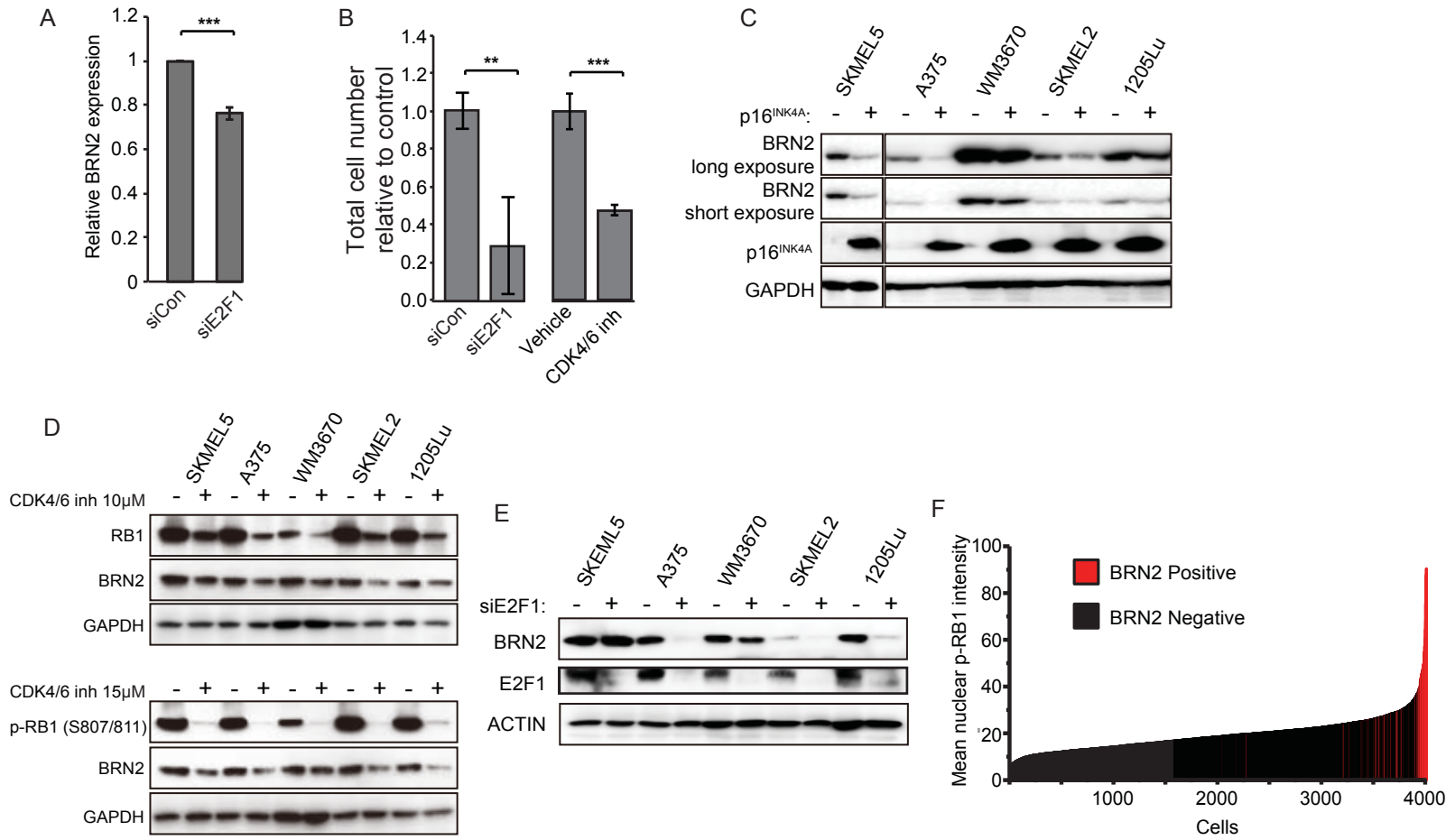

Figure S6. Downstream effects of CDK4/6 signaling, Related to Figure 7. (A) RT-qPCR quantification of BRN2 mRNA levels in three *CDKN2A* null NHMs treated siRNA targeting E2F1. Values are relative to matched engineered NHMs treated with control non-targeting siRNA (siCon). (B) Total relative cell number of the cell populations analyzed in Figure 7E-F after indicated treatment or transfection. (C) Representative western blot of five *CDKN2A* null or silenced human melanoma lines with or without overexpression of $p16^{INK4A}$. Two exposures of BRN2 are shown to visual different baseline levels. (D) Representative western blot of five *CDKN2A* null or silenced human melanoma lines with or without treatment with indicated concentrations of CDK4/6 inhibitor. (E) Representative western blot of five *CDKN2A* null or silenced human melanoma lines with or without siRNA targeting E2F1. (F) Quantification of eight cases stained as in Figure 7I. All nuclei (n=4011) identifiable by DAPI were ranked by intensity of nuclear phospho-RB1 signal. Cells that were positive for BRN2 are indicated in red. All error bars represent standard deviation of the mean. Asterisks indicate p-values of ** <0.005 to *** <0.0005 from unpaired t-test.